Fluid-Phase Connectivity and Translational Diffusion in a Eutectic, Two-Component, Two-Phase Phosphatidylcholine Bilayer†

Thomas Bultmann,‡ Winchil L. C. Vaz,*,‡ Eurico C. C. Melo,‡,§ Robert B. Sisk,∥ and Thomas E. Thompson∥

Max-Planck-Institut für Biophysikalische Chemie, Postfach 2841, D-3400 Göttingen, FRG, and Department of Biochemistry and Biophysics Program, University of Virginia, Charlottesville, Virginia 22908

Received December 31, 1990; Revised Manuscript Received March 11, 1991

ABSTRACT: In recent work [Vaz, W. L. C., Melo, E. C. C., & Thompson, T. E. (1989) *Biophys. J. 56*, 869–876] we have shown that translational diffusion studies using fluorescence recovery after photobleaching (FRAP) provide information concerning domain structures and fluid-phase connectivity in lipid bilayers in which solid and fluid phases coexist. In the present paper, translational diffusion of the fluid-phase-soluble, solid-phase-insoluble fluorescent lipid derivative *N*-(7-nitrobenzoxa-2,3-diazol-4-yl)dilauroylphosphatidylethanolamine and the fluid-phase connectivity are examined in lipid bilayers prepared from binary mixtures of 1-docosanoyl-2-dodecanoylphosphatidylcholine ($C_{22:0}C_{12:0}$PC) and 1,2-diheptadecanoylphosphatidylcholine (di-$C_{17:0}$PC) by using FRAP. The phosphatidylcholine mixture used provides a eutectic system with a eutectic point at a composition of about 0.4 mole fraction of di-$C_{17:0}$PC and a temperature of about 37 °C [Sisk, R. B., Wang, Z. Q., Lin, H. N., & Huang, C. H. (1990) *Biophys. J. 58*, 777–783]. Two regions in temperature and composition, respectively below and above 0.4 mole fraction of di-$C_{17:0}$PC, where fluid and solid phases coexist in the same lipid bilayer, are available for examination of fluid-phase connectivity. In mixtures containing <0.4 mole fraction of di-$C_{17:0}$PC the fluid phase coexists with a mixed interdigitated L_c gel phase composed mostly of $C_{22:0}C_{12:0}$PC, whereas in mixtures containing >0.4 mole fraction of di-$C_{17:0}$PC the fluid phase coexists with a $P_{\beta'}$ gel phase mostly composed of di-$C_{17:0}$PC. When the solid phase is a $P_{\beta'}$ gel phase, the temperature of fluid-phase connectivity for the mixtures lies close to the fluidus, which means that a small (≈20%) mass fraction of solid phase can divide the large bulk of the bilayer that is fluid into nonconnected domains. A reticular structure is inferred for the continuous $P_{\beta'}$ gel phase domain in this case. When the solid phase is a mixed interdigitated L_c gel phase, the temperature of fluid-phase connectivity for the mixtures lies almost at the solidus, which means that a very small (≤10%) mass fraction of fluid phase forms a continuous domain even when the large bulk of the bilayer is in a solid phase. This implies a reticular structure for the fluid phase and an insular structure for the L_c gel phase domains in the system. We try to understand the result in terms of continuum percolation models and discuss possible domain structures in these lipid bilayers.

Biological membranes are made up principally of a lipid bilayer that acts as a two-dimensional solvent sheet in which (integral) proteins are dissolved or to which (extrinsic) proteins are adsorbed. The lipid bilayer is usually visualized as a mostly fluid matrix made up of a complex mixture of amphipathic lipids (Singer & Nicolson, 1972). The composition of each monolayer in the lipid bilayer is distinct from that of the apposing monolayer, and this compositional difference is rigidly maintained in most biological membranes (Op den Kamp, 1979). The fact that the bilayer is a mixture of often very different chemical species whose only similarity lies in their amphiphilicity suggests the existence of distinct phases in each monolayer dependent upon temperature, chemical composition, lateral pressure, and, for bilayers with charged lipid species, ionic composition and pH of the bounding aqueous phase. This expectation is further accentuated by the complex polymorphism of hydrated lipid systems in the lyotropic and thermotropic regimes (Cevc & Marsh, 1987; Jain, 1988; Gennis, 1989). The existence of domain structures in biological membranes has been demonstrated in a variety of systems [for reviews see Klausner and Kleinfeld (1984) and Tocanne et al. (1989)]. Quite recently, lipid domains in erythrocyte membranes have been directly observed by digitized fluorescence microscopy (Rodgers & Glaser, 1991).

Studies on lipid bilayer systems composed of more than one lipid species have shown that the component lipids in general exhibit large deviations from ideal mixing (Cevc & Marsh, 1987). This implies that the complex mixtures encountered in biological membranes may form a mosaic of stable and coexisting domains whose chemical and physical properties are distinct from each other. The coexistence of lipid phases in the plane of the biological membrane can have several consequences for membrane-localized processes. Significant effects upon in-plane diffusion in the membrane and reactions that are limited by such diffusion may be expected as a result of simple physical–chemical barriers such as solubility barriers resulting from preferential solvation of proteins, or other reactive lipophilic membrane components, by one or a combination of lipid species in separated phases, or from a coexistence of solid (ordered) and fluid (disordered) or charged and uncharged lipid phases. If a bilayer is poised near a transition boundary in the phase diagram, a small change in chemical composition or some other pertinent physical parameter can effect a large change in the phase composition and domain structure of the membrane and thereby signifi-

† This work was supported in part by Grants GM-14628 and GM 23573 from the National Institutes of Health and Grant DiR-8907318 from the National Science Foundation.

‡ Max-Planck-Institut für Biophysikalische Chemie.

§ Permanent address: Centro de Tecnologia Química e Biológica, P-2780 Oeiras, Portugal.

∥ University of Virginia.

0006-2960/91/0430-5573$02.50/0

cantly influence its biochemical response. In the extreme case these changes may act as switching mechanisms in the physiology of the cell and its response to its environment.

We have recently undertaken the study of long-range translational diffusion of a fluid-phase-soluble, solid-phase-insoluble fluorescent phospholipid derivative, using the fluorescence recovery after photobleaching (FRAP)[1] technique, in lipid bilayers under conditions where solid (ordered or gel) and fluid (disordered or liquid crystalline) phases coexist in the same bilayer (Vaz et al., 1989, 1990). The aim has been to understand under what conditions the fluid phase is continuous and the solid phase discontinuous (and vice versa) in a lipid bilayer where the two phases coexist laterally in the membrane. The results have allowed the definition of a threshold for percolation in the fluid phase as a function of the temperature and composition for peritectic (Vaz et al., 1989) and isomorphous (Vaz et al., 1990) phosphatidylcholine mixtures in multilayers. In this paper we report our results of similar studies on bilayers formed from a eutectic mixture of 1-docosanoyl-2-dodecanoylphosphatidylcholine ($C_{22:0}C_{12:0}PC$) and diheptadecanoylphosphatidylcholine (di-$C_{17:0}PC$) whose phase behavior as a function of temperature and composition at constant pressure and in the excess water regime has been recently reported (Sisk et al., 1990).

Materials and Methods

Di-$C_{17:0}PC$ was purchased from Avanti Polar Lipids, Inc., Pelham, AL. $C_{22:0}C_{12:0}PC$ was synthesized as described by Lin et al. (1990). NBD-DLPE was synthesized as described by Vaz and Hallmann (1983). All lipids were checked to be free of lysolipid and fatty acid impurities by thin-layer chromatography and stored at −20 °C as the dry material or as chloroform solutions for shorter periods.

Preparation of Multibilayers. The lipids were dissolved in chloroform at a concentration of 10^{-2} M, and these solutions were mixed to give the desired PC mixture with about 2–3 mg of total lipid containing 0.001 mole fraction of NBD-DLPE. The mixture was allowed to stand at room temperature for 30 min, and the solution was then evaporated to a volume of 0.05–0.1 mL by blowing a stream of nitrogen over it. The concentrated solution was deposited on a siliconized glass microscope slide warmed to 90 °C on a hot plate, taking care that the lipid residue did not spread over an area >1 cm^2. After most of the solvent had evaporated on the hot plate, the slide with the residue was placed in a vacuum desiccator over anhydrous calcium chloride granules for at least 3 h and then warmed in an oven at 70 °C for an additional 10 min. The dry lipid residue was hydrated at 70 °C by dropping a cover slip with a hanging drop of 70 μL of 0.01 M sodium phosphate buffer, pH 7.5, containing 0.05 M potassium chloride and 0.02% sodium azide. The buffer was preheated to 70 °C. In some experiments the dried lipid residue on the slide was first exposed to an atmosphere with a relative humidity close to 100% at 70 °C for 6 h before it was covered with the cover slip and the hanging drop of buffer. No differences in the FRAP results on samples prepared in either way were detected, so the vapor-hydration step was omitted to avoid excessively long exposures of the hydrated lipid mixtures to high temperatures. Hydration was done at 70 °C in order to be at a temperature well above the main phase-transition temperatures (T_m) of both constituents of the binary phosphatidyl choline mixture (T_m is 43.4 °C for $C_{22:0}C_{12:0}PC$ and 49.0 °C for di-$C_{17:0}PC$). After hydration with buffer, the slides were left in a humid atmosphere at 70 °C for 30 min followed by a further 2 h at 50–55 °C and then gradually cooled down to 20 °C over a 4-h period. Before FRAP measurements the slide was sealed with a silicone paste (Bayer AG, Leverkusen, FRG) to prevent evaporation of water. All samples were examined by polarized light microscopy to ensure that only optically uniaxial multilayers of large area were studied. Some samples were checked for formation of lysolipids after the FRAP experiments; none were detected.

FRAP Experiments. FRAP experiments were performed by using a uniform circular beam profile [see Axelrod et al. (1976)] with a radius of 3 μm obtained by using a Zeiss Neofluar 10/0.3 objective lens. Instrumental details have been described in a previous paper (Vaz et al., 1989). First a cooling and then a heating curve was measured on each sample. In measuring cooling curves the samples (sealed microscope slides) were first heated to 52 °C on the microscope stage, which has a Peltier temperature control unit (Cambridge Thermionic Corp., Cambridge, MA) built into it, and then cooled gradually to 30 °C in steps of 1 °C, keeping the sample for at least 30 min between two successive temperatures. FRAP measurements were made at convenient temperature intervals in this range. After the sample had been cooled to 30 °C it was placed in a closed chamber over distilled water at 20 °C and left in the dark for a period of at least 3 days before the heating curves were measured. Heating curves were essentially a reversal of the cooling curves, starting at 30 °C and heating up to a temperature just above the fluidus for the mixture being examined.

FRAP measurements used the 488-nm line output of an argon ion laser (Spectra Physics, Mountain View, CA) at 100–300 mW. Each curve was collected in a total of 1000 channels with a minimum period of 30 ms/channel. Ten percent of the channels were recorded before turning on the photobleaching pulse. Bleaching times were never longer than 1 channel time. The monitoring beam intensity was chosen such that no measurable photobleaching could be observed due to exposure to the monitoring beam alone over a period equivalent to the time required to obtain a typical FRAP curve. The recovery curves were fitted to the equations given by Soumpasis (1983) as described previously (Vaz et al., 1989) by using the Simplex algorithm (Quantum Chemistry Exchange Program, J. P. Chandler, Oklahoma State University, Stillwater, OK). In cases where the recovery could not be well described as resulting from a single diffusing component, recoveries were analyzed as being due to single diffusing components superimposed upon linear ramps. The linear ramp reflects the initial recovery phase(s) for recovery due to one or more diffusing components with very much slower characteristic recovery times. In the fitting procedure, the characteristic recovery time, τ, the slope of the linear ramp, the fluorescence intensity immediately after photobleaching, $F(0)$, and the fluorescence intensity at infinite time after photobleaching, $F(\infty)$, were adjustable. The fluorescence intensity prior to photobleaching, $F(i)$, was taken as the mean value of 100 channels measured before the photobleaching pulse.

Results

Temperature–Composition Phase Diagram for the Mixture of $C_{22:0}C_{12:0}PC$ and Di-$C_{17:0}PC$. The phase diagram for the mixture as obtained from differential scanning calorimetric

[1] Abbreviations: di-$C_{17:0}PC$, 1,2-diheptadecanoylphosphatidylcholine; $C_{22:0}C_{12:0}PC$, 1-docosanoyl-2-dodecanoylphosphatidylcholine; DMPC, dimyristoylphosphatidylcholine; DPPC, dipalmitoylphosphatidylcholine; DSPC, distearoylphosphatidylcholine; FRAP, fluorescence recovery after photobleaching; NBD-DLPE, *N*-(7-nitrobenzoxa-2,3-diazol-4-yl)dilauroylphosphatidylethanolamine; T_m, main lipid bilayer phase transition temperature.

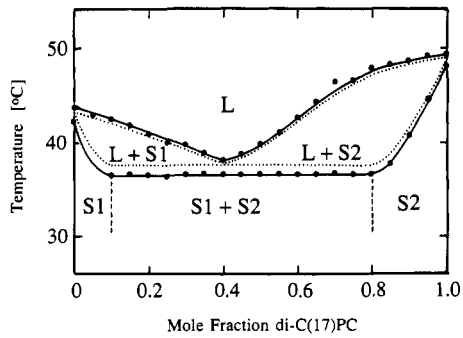

FIGURE 1: Temperature–composition phase diagram for a mixture of di-$C_{17:0}$PC and $C_{22:0}C_{12:0}$PC. The solid line and points show the experimentally determined calorimetric onset and completion temperatures; the dotted line is the phase diagram after correction for the finite widths of the phase transitions of the pure components. The areas in the phase diagram are labeled to indicate a liquid phase (L), a solid phase predominantly composed of $C_{22:0}C_{12:0}$PC (S1), a solid phase predominantly composed of di-$C_{17:0}$PC (S2), and regions where these phases coexist.

studies in shown in Figure 1 with and without correction for the finite widths of the phase transitions of the pure components. This phase diagram has been obtained and discussed in some depth by Sisk et al. (1990). Only the details relevant to this work will be discussed here. The mixture is a typical eutectic with a eutectic point at about 0.4 mole fraction of di-$C_{17:0}$PC and a eutectic horizontal at 36.5 °C (uncorrected; 37.7 °C corrected). For compositions below 0.4 mole fraction of di-$C_{17:0}$PC, where solid and fluid phases coexist, the solid phase is a mixed interdigitated L_c phase whose main component is $C_{22:0}C_{12:0}$PC. For compositions above 0.4 mole fraction of di-$C_{17:0}$PC and at temperatures where solid and fluid phases coexist, the solid phase is a $P_{\beta'}$ phase whose main component is di-$C_{17:0}$PC. The two solid phases are mutually immiscible and coexit as a mechanical mixture below the eutectic horizontal. This mixture, therefore, provides two regions in the temperature–composition phase diagram where solid and fluid phases coexist, the solid phases having different physical characteristics in each case.

FRAP Experiments. In the FRAP experiments we have used *N*-(7-nitrobenzoxa-2,3-diazol-4-yl)dilauroylphosphatidylethanolamine (NBD-DLPE) as the fluorescent lipid test molecule whose long-range translational diffusion is examined. As discussed in previous work (Vaz et al., 1989, 1990), this lipid derivative partitions exclusively into the lipid fluid phase in bilayers where solid and fluid phases coexist. This preferential partitioning of NBD-DLPE into fluid domains has also been shown in monolayers (R. Tillmann, H. E. Gaub, and W. L. C. Vaz, manuscript in preparation).

Figure 2 shows some typical FRAP curves obtained on multibilayers formed from mixtures of $C_{22:0}C_{12:0}$PC and di-$C_{17:0}$PC containing 0.001 mole fraction of NBD-DLPE at different temperatures. FRAP curves obtained on multibilayers of pure $C_{22:0}C_{12:0}$PC and pure di-$C_{17:0}$PC also containing 0.001 mole fraction of NBD-DLPE are also shown for reference. In all the multibilayers examined in the fluid phase, the FRAP curves show a rapid fluorescence recovery, which can be attributed to a single diffusing component (Figure 2A). In multibilayers in the $P_{\beta'}$ phase (pure di-$C_{17:0}$PC at 45 °C, Figure 2B), the fluorescence recovery is due to more than one diffusional process, which can be divided into two classes: a fast-recovering component and one or more very slowly re-

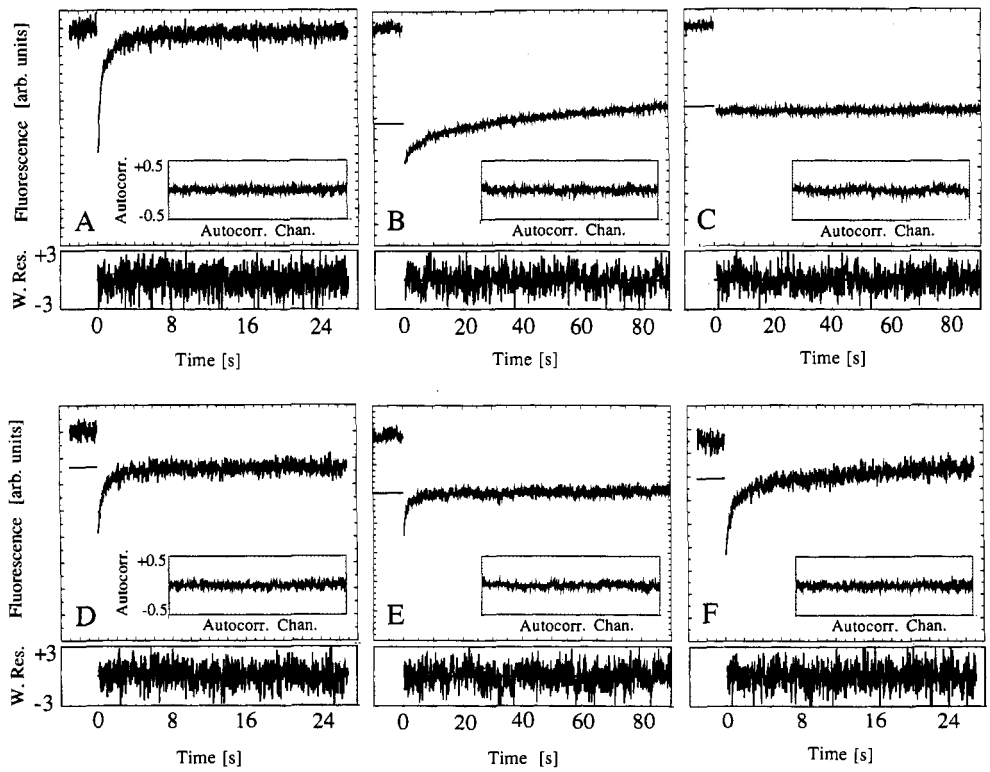

FIGURE 2: Typical FRAP recovery curves for NBD-DLPE in multibilayers. (A) Pure di-$C_{17:0}$PC at 52.3 °C. The best fit was obtained with τ = 0.21 s, slope = 0.0 counts/s, and 99% recovery; χ^2 = 1.5. (B) Pure di-$C_{17:0}$PC at 44.8 °C. The best fit was obtained with τ = 5.2 s, slope = 9.7 counts/s, and 32% recovery; χ^2 = 1.2. (C) Pure $C_{22:0}C_{12:0}$PC at 30.1 °C. The fit shown was obtained with τ = 200 s, slope = 0.0 counts/s, and 100% recovery; χ^2 = 1.1. The short recovery time examined in the experiment and shown in the figure does not allow reliable estimation of fitting parameters. Experiments done over longer recovery periods did not show recovery either. (D) Pure $C_{22:0}C_{12:0}$PC at 41.8 °C. The fit shown was obtained with τ = 0.28 s, slope = 0.0 counts/s, and 71% recovery; χ^2 = 1.2. (E) Mixture of di-$C_{17:0}$PC and $C_{22:0}C_{12:0}$PC (17.6/82.4, mol/mol) at 35.0 °C. The best fit was obtained with τ = 0.41 s, slope = 0.4 counts/s, and 52% recovery; χ^2 = 1.2. (F) Mixture of di-$C_{17:0}$PC and $C_{22:0}C_{12:0}$PC (80/20, mol/mol) at 43.2 °C. The best fit was obtained with τ = 0.41 s, slope = 3.9 counts/s, and 52% recovery; χ^2 = 1.3. The inserts and bottom panels show plots of the autocorrelation functions and the weighted residuals in standard deviation units.

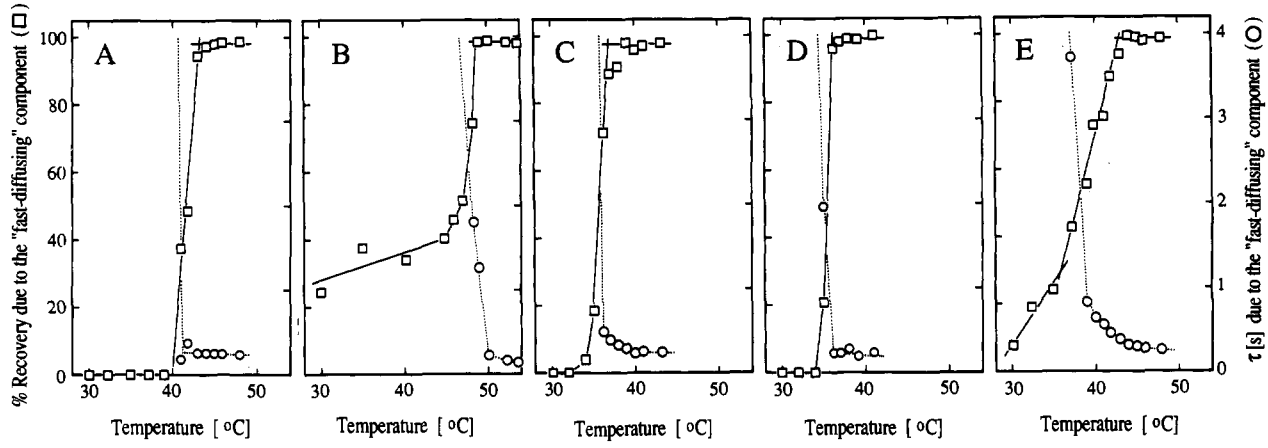

FIGURE 3: Fluorescence recovery and characteristic recovery times as a function of temperature for NBD-DLPE in multibilayers. (A) Pure $C_{22:0}C_{12:0}PC$. (B) Pure di-$C_{17:0}PC$. (C) Mixture of di-$C_{17:0}PC$ and $C_{22:0}C_{12:0}PC$ (17.6/82.4, mol/mol). (D) Mixture of di-$C_{17:0}PC$ and $C_{22:0}C_{12:0}PC$ (40/60, mol/mol). (E) Mixture of di-$C_{17:0}PC$ and $C_{22:0}C_{12:}PC$ (70/30, mol/mol).

covering processes whose characteristic recovery times, τ, are at least 1 order of magnitude larger than the recovery time for the fast component. As discussed elsewhere (Vaz et al., 1989), we have fit these curves to an incompletely recovering fast-diffusing component superimposed upon a linear ramp that simulates the initial phase of recovery due to the slow process(es). The fast recovery is attributed to quasi-one-dimensional diffusion of the probe in dislocation defects in the gel phase (Derzko & Jacobson, 1980; Schneider et al., 1983), and its amplitude is related to the extent to which these defects are connected over dimensions comparable to the diameter of the illuminated spot in the FRAP experiments (6 μm). The slowly diffusing component (or components) probably reflects diffusion of probe trapped in gel-phase domains or the rate at which probe molecules cross a gel-phase barrier between two paths where there is rapid diffusion. In lipid multibilayers in the mixed interdigitated L_c phase ($C_{22:0}C_{12:0}PC$ at 30 °C, Figure 2C), no fluorescence recovery is seen over the time scale of the experiment. At temperatures very close to the phase transition temperature ($C_{22:0}C_{12:0}PC$ at 42 °C, Figure 2D), an incomplete fast recovery begins to appear, the extent of recovery increasing with approach to the phase transition temperature. Apparently the dislocation defects to which the fast recovery may be attributed are interconnected over large distances only very close to the phase transition in this mixed interdigitated L_c phase.

FRAP curves obtained on mixtures of $C_{22:0}C_{12:0}PC$ and di-$C_{17:0}PC$ containing $\leq$0.4 mole fraction of di-$C_{17:0}PC$ at temperatures where the bilayers are fully in the gel phase are similar to those seen for pure $C_{22:0}C_{12:0}PC$ bilayers in the L_c phase (see Figure 2C). The transition to diffusion in a fully connected fluid phase, however, occurs over a wider range of temperatures. Bilayers having compositions containing >0.4 mole fraction of di-$C_{17:0}PC$ show a small fast recovering fraction similar to that seen in $P_{\beta'}$-phase pure di-$C_{17:0}PC$ multibilayers at the same temperature (see Figure 2B). In the region of the phase diagram where solid and fluid phases coexist, part of the recovery in the FRAP curves is due to a fast-diffusing component and the other part is due to one or more slower diffusion processes whose characteristic recovery times are very slow compared to that of the fast component (Figure 2E,F). On the time scales of the FRAP curves shown here, we only see the very beginning of the slow recovery processes, which permits us to approximate these recoveries with a linear ramp, as discussed above. The fast-recovering component is understood as being due to diffusion in fluid domains in the bilayers. Its amplitude is related to the size of the fluid domains relative to the spot size and also to the extent to which the fluid domains are connected with each other by fluid paths. Figure 2E shows a typical FRAP curve for a mixture with $\leq$0.4 mole fraction of di-$C_{17:0}PC$ in the temperature range of coexisting solid and fluid phases. The slow-recovering process(es) account for a very small fraction of the recovery obtained over the period of measurement. For mixtures containing >0.4 mole fraction of di-$C_{17:0}PC$ in the solid–fluid coexistence temperature range (Figure 2F) the slow process (or processes) accounts for a substantially larger fraction of the fluorescence recovery. This may be related to the differences in diffusion in the L_c phase compared to the $P_{\beta'}$ phase discussed above.

Fluid Phase Connectivity. For a given bilayer composition we define that temperature at which complete fluorescence recovery can be attributed to a single fast-diffusing component as the temperature of fluid-phase connectivity at that composition (Vaz et al., 1989). For pure lipid bilayers this temperature is about the same as the gel–liquid crystalline phase transition temperature. In mixed lipid bilayers, where solid and fluid phases can coexist over a wide range of temperatures, fluid-phase connectivity has been observed at temperatures close to the fluidus in the phase diagram of DMPC/DSPC mixtures (Vaz et al., 1989) or at temperatures where the mass fractions of solid and fluid phases are about equal in DMPC/DPPC mixtures (Vaz et al., 1990). Figure 3 shows the percent recovery of fluorescence after photobleaching and the characteristic recovery times, τ, as a function of temperature for pure $C_{22:0}C_{12:0}PC$ (Figure 3A), pure di-$C_{17:0}PC$ (Figure 3B) and various mixtures of these lipids (Figure 3C–E). Only the heating curves are presented since no hysteresis was observed between the heating and cooling curves. In bilayers of pure $C_{22:0}C_{12:0}PC$ (Figure 3A) in the L_c phase, no fluorescence recovery after photobleaching was observed until about 41 °C. At this temperature a rapid ($\tau \approx 0.25$ s) but partial (% recovery $\approx$ 50%) recovery of the photobleached fluorescence is obtained. At $T \geq 43$ °C, the recovery of fluorescence is complete and due to a single fast-diffusing component ($\tau \leq 0.25$ s), which is very typical for diffusion in L_α-phase lipid bilayers (Vaz et al., 1985). The main phase transition temperature, T_m, for $C_{22:0}C_{12:0}PC$ bilayers is 43.4 °C (Huang, 1989). In bilayers of pure di-$C_{17:0}PC$ (Figure 3B) a slightly different pattern is seen. In the gel phase of these bilayers between 30 and 49 °C there is a partial recovery of fluorecence (20–50%) with $\tau \geq 5$ s ("fast"-recovering component) superimposed on a linear ramp that represents the initial recovery phase of one or more very slow diffusion

Table I: Temperature of Fluid-Phase Connectivity for Different Mixtures of $C_{22:0}C_{12:0}PC$ and di-$C_{17:0}PC$ Examined in This Work

mole fraction of di-$C_{17:0}PC$	temperature of fluid-phase connectivity[a] (°C)
0.0	43.1
0.10	36.9
0.176	37.0
0.25	36.8
0.40	36.6
0.60	40.0
0.70	43.0
0.80	44.2
0.90	47.0
1.00	48.3

[a] From heating curves.

processes. Above T_m [≈49.0 °C (Huang, 1989)] there is a transition to typical diffusion behavior seen in L_α-phase lipid bilayers (100% recovery with $\tau \leq 0.24$ s).

Figure 3C shows the percent recoveries and τ values as a function of temperature for a mixture of $C_{22:0}C_{12:0}PC$ and di-$C_{17:0}PC$ containing 0.176 mole fraction of di-$C_{17:0}PC$. At $T < 34$ °C no fluorescence recovery is seen after photobleaching in these bilayers. This is similar to the result seen in bilayers made from pure $C_{22:0}C_{12:0}PC$ below T_m. Between 34 and 37 °C a fast component appears whose amplitude increases with increasing temperature until at about 37 °C 100% recovery of fluorescence after photobleaching is observed and accounted for by a single diffusing component with a τ value similar to that typically seen for diffusion in a fluid lipid bilayer. Thus, for this mixture the fluid phase is continuous at temperatures very close to the solidus (see Figure 1), where the mass of the fluid phase is ≤10% of the mass of the system. This sort of behavior was seen in all mixtures having ≤0.4 mole fraction of di-$C_{17:0}PC$. Figure 3D shows the behavior in a mixture containing 0.4 mole fraction of di-$C_{17:0}PC$, a composition very close to the eutectic point.

Figure 3E shows the percent recovery and τ values obtained from FRAP experiments on a mixture containing 0.7 mole fraction of di-$C_{17:0}PC$. In the temperature range of solid–fluid coexistence at this composition, the solid phase is composed primarily of di-$C_{17:0}PC$ (see Figure 1). In this mixture, at temperatures below 37 °C (gel phase), the fluorescence recovery curves are composed of a "fast"-recovering component superimposed on one or more very slowly recovering processes whose initial portions are approximated here as a linear ramp (see description associated with Figure 2B,F). The "fast" component with $\tau \approx 5$–10 s accounts for between 5 and 25% of the fluorescence recovery. Above 37 °C the fractional recovery due to the fast component increases rapidly until about 43 °C, above which temperature all of the recovery is due to a single diffusing component with recovery times that are characteristic of diffusion in a continuous fluid phase. When compared with the phase diagram (Figure 1), the temperature of fluid-phase connectivity in this mixture is very close to the liquidus, unlike the behavior described above for mixtures containing ≤0.4 mole fraction of di-$C_{17:0}PC$. However, this behavior is quite similar to that reported by us earlier for the peritectic mixture of DMPC/DSPC (Vaz et al., 1989).

Thus, in bilayers formed from mixtures of $C_{22:0}C_{12:0}PC$ and di-$C_{17:0}PC$ when solid and fluid phases coexist, fluid-phase connectivity is either obtained at a low mass fraction of fluid in the system (mixtures containing ≤0.4 mole fraction of di-$C_{17:0}PC$) when the coexisting solid phase is a mixed interdigitated L_c phase or at a high mass fraction of fluid in the system (mixtures containing >0.4 mole fraction of di-$C_{17:0}PC$)

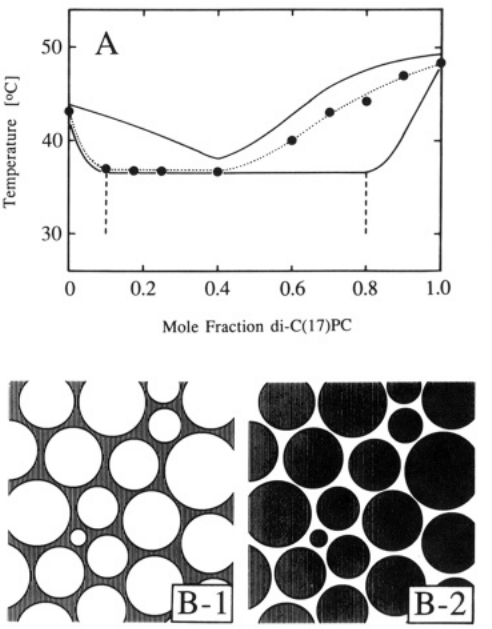

FIGURE 4: (A) Points of fluid-phase connectivity obtained in this work (large solid circles) plotted on the uncorrected temperature–composition phase diagram for the mixture of di-$C_{17:0}PC$ and $C_{22:0}C_{12:0}PC$. (B) Schematic diagram demonstrating extremes of phase structures. (1) A continuous fluid phase (hatched area) disconnects a gel phase (clear area) corresponding to the situation immediately above in (A) for the two-phase area at concentration <0.4 mole fraction of di-$C_{17:0}PC$. (2) A continuous gel phase (clear area) disconnects a fluid phase (hatched area). This corresponds to the situation directly above in (A) for the two-phase region and concentrations >0.4 mole fraction of di-$C_{17:0}PC$.

when the coexisting solid phase is a $P_{\beta'}$ phase. The temperatures of fluid-phase connectivity for the different compositions examined in this work are given in Table I. These values, when plotted on the temperature–composition phase diagram for the system as in Figure 4, define a line in the phase diagram that is related to the percolation threshold for the two-phase system under consideration. At temperatures above this line the fluid phase is a continuous phase in the system and the solid phase is discontinuous, whereas below this line the opposite is true.

Discussion

In order to understand fluid-phase connectivity in this system, let us assume the shapes, dimensions, and positions of the coexisting domains of solid and fluid phases to be static in the time frame of the FRAP experiment. In that portion of the phase diagram containing >0.4 mole fraction of di-$C_{17:0}PC$, fluid-phase connectivity occurs at low mass fractions of solid phase. This is possible only if the solid phase forms a two-dimensional reticulum in the plane of the bilayer. It is this condition that was found over much of the peritectic system DMPC/DSPC (Vaz et al., 1989). A solid-phase reticulum could be the result of preferential growth along one of the two orthogonal directions in the plane of the bilayer. In contrast to this situation, at concentrations of di-$C_{17:0}PC$ <0.4 mole fraction, fluid-phase connectivity occurs at low mass fractions of fluid phase. This is possible only if the solid phase in the system forms generally centrosymmetric structures that permit the existence of a reticulum of fluid-phase channels. A simplified picture of these two extremes of phase structure is shown in Figure 4B-1,2. Panel 4B-1 depicts the situation below 0.4 mole fraction of di-$C_{17:0}PC$, and panel 4B-2 depicts the situation above that concentration.

The fluid-phase connectivity for concentrations >0.4 mole

fraction of di-$C_{17:0}$PC can be viewed as a problem of continuum percolation in two dimensions (Xia & Thorpe, 1988). These authors compute the percolation concentration for identical ellipses in a two-dimensional plane where both the ellipse centers and orientations are random and overlapping of ellipses is allowed. If the gel-phase domains are modeled as elliptical structures of uniform area and axial ratio with random orientations, the percolation threshold (defined as the minimum fractional area of fluid phase in the system at which the fluid is still continuous) will depend on the axial ratio of the ellipses. It varies between 0.33 for circular shapes and 1.0 for needle-like shapes. Values of the percolation threshold as a function of the axial ratio, b/a, for elliptical domains, where a and b are the major and minor semiaxes of the ellipses, are calculated by Xia and Thorpe (1988). There is, however, a priori no reason to expect the gel domains to be of equal area. One would expect the percolation threshold to be even lower if the solid domains were of random sizes but of the same shape. When the calculations of Xia and Thorpe (1988) are applied to mixtures of $C_{22:0}C_{12:0}$PC and di-$C_{17:0}$PC at concentrations >0.4 mole fraction of di-$C_{17:0}$PC, the ratio b/a is found to lie between 0.1 and 0.25, depending upon the concentration of the phospholipid components. It is not difficult to imagine the gel phase reticulum illustrated in Figure 4B-2 to be made up of roughly elliptical segments of different sizes. It is interesting to note that solid-phase domains appear to be less eccentric (b/a closer to 1.0) when, upon heating, the system enters the two-phase region from a single gel phase. Extreme elliptical domains are found when the system, upon heating, enters the two-phase region from a region of coexisting gel phases that are mutually immiscible. A similar result was also noted in our earlier work (Vaz et al., 1989, 1990). We as yet have no explanation for these observations.

The continuum percolation model discussed above can be extended to the concentration region at mole fractions of di-$C_{17:0}$PC < 0.4 by noting, as pointed out by Xia and Thorpe (1988), that in a two-dimensional system when the fluid phase disconnects, the solid phase connects and vice versa. That is, there is a single percolation point at a given system concentration. In higher dimensional systems this is not the case. Thus the elliptical domains previously considered to be gel structures can equally well, in a formal sense, be considered to be fluid domains. We estimate the fractional area of fluid phase at connectivity in the concentration regime to be ≤0.1. Hence the fluid regions are a connected network of needlelike domains—a reticulum. Obviously from this viewpoint the gel domains will be of unspecified average size and shape. In the one extreme they could be circular, but of varying size, as suggested above and depicted in Figure 4B-1.

The discussion thus far has assumed the phase domain structure to be static in the time frame of the FRAP measurement. There are, however, two dynamic aspects of the phase structure that may influence the translational diffusion of the fluorescent probe. The first is the lateral diffusion of disconnected solid domains in a continuous fluid phase near connectivity. If the diffusion coefficient of these domains and the diffusion coefficient of the probe in the plane of the bilayer are of comparable magnitudes, this will affect the time course of recovery at temperatures above, but near, the temperature at which connectivity occurs. This effect is, however, likely to be small (Saxton, 1982). The second dynamic event is local fluctuational melting and solidification of gel domains. Obviously, if the reticular areas of gel domains block lateral diffusion of fluorescent probe molecules, the transient development of fluid paths by melting will allow the probes occasionally to pass the barrier. If the frequency of hole formation in the gel-phase barrier is high compared to the diffusion rate of the probe, connectivity will be operationally obtained at a higher mass fraction of gel phase than would be the case for a static-phase structure. In terms of the FRAP experiment, fluctuations in phase structure of this type will cause the observed temperature of connectivity to be lower than it would be if the phase structure were static. The percolation problem with fluctuating barriers has been discussed in some detail by Saxton (1990). At the present time we do not know the magnitude of the contribution of these dynamic effects to our measurements.

Whether the solid phase forms a reticular domain structure that blocks percolation in the lipid bilayer even when the fluid phase is the larger mass fraction of the system or whether it forms a reticular fluid phase with centrosymmetric gel domains evidently depends upon the type of gel-phase structure of the major component in the solid phase. On the basis of our results obtained thus far [see also Vaz et al. (1989, 1990)], it seems probably that the $P_{\beta'}$ gel phase leads to a reticular domain system, whereas a mixed interdigitated L_c phase such as that formed by $C_{22:0}C_{12:0}$PC used in this work leads to the formation of centrosymmetric gel domains. The consequences for diffusion-controlled reactions that take place between membrane components in bilayers in which solid and fluid domains coexist are different for the two types of gel-phase domains discussed here. The insular gel phases will act as obstacles in the path of a diffusing molecule, thereby making the diffusion coefficient distance-dependent (Saxton, 1982, 1987, 1989). In the case of effectively reticular gel-phase domains or domain aggregates, a small mass fraction of gel phase in the membrane may subdivide the fluid phase into the nonconnected areas, thereby reducing reactant contact during the lifetime of the gel-phase reticulum. From our results it appears that gel-phase reticular structures may be long-lived on the time scale of the FRAP experiments (minutes). If a biological membrane exists close to the percolation threshold, then small changes in lipid composition, lateral pressure, or surface ionic conditions could very rapidly shift the membrane bilayers from a connected to a nonconnected state (or vice versa) and act as a rapid switching mechanism controlling lateral interactions between membrane components. It is not clear at this time that solid–fluid phase separations do occur universally in biological membranes. However, the important consequences that such phase separations could have for membrane physiology may make the search for them well worth the while.

Acknowledgments

We thank Dr. Thomas M. Jovin for his continued support of this work and Dr. Rod Biltonen, Dr. Ching-hsien Huang, and Paulo Almeida for stimulating discussions of it.

Registry No. $C_{22:0}C_{12:0}$PC, 126959-05-5; di-$C_{17:0}$PC, 67896-64-4.

References

Axelrod, D., Koppel, D. E., Schlessinger, J., Elson, E., & Webb, W. W. (1976) *Biophys. J. 16*, 1055–1069.

Cevc, G., & Marsh, D. (1987) *Phospholipid Bilayers*, John Wiley & Sons, New York.

Derzko, Z., & Jacobson, K. (1980) *Biochemistry 19*, 6050–6057.

Gennis, R. B. (1969) *Biomembranes: Molecular Structure and Function*, Springer-Verlag, New York.

Huang, C. H. (1989) *Klin. Wochenschr. 68*, 149–165.

Jain, M. K. (1988) *Introduction to Biological Membranes*, 2nd ed., John Wiley & Sons, New York.

Klausner, R. D., & Kleinfeld, A. M. (1984) In *Cell Surface Dynamics* (Perelson, A. S., De Lisi, C., & Wiegel, F. W., Eds.), pp 23–58, Marcel Dekker, Inc., New York.
Lin, H. N., Wang, Z. Q., & Huang, C. H. (1990) *Biochemistry 29*, 7063–7072.
Op den Kamp, J. A. F. (1979) *Annu. Rev. Biochem. 48*, 47–71.
Rodgers, W., & Glaser, M. (1991) *Proc. Natl. Acad. Sci. U.S.A. 88*, 1364–1368.
Saxton, M. J. (1982) *Biophys. J. 39*, 165–173.
Saxton, M. J. (1987) *Biophys. J. 52*, 989–997.
Saxton, M. J. (1989) *Biophys. J. 56*, 615–622.
Saxton, M. J. (1990) *Biophys. J. 57*, 1167–1177.
Schneider, M. B., Chan, W. K., & Webb, W. W. (1983) *Biophys. J. 43*, 157–165.
Singer, S. J., & Nicolson, G. L. (1972) *Science 175*, 720–731.
Sisk, R. B., Wang, Z. Q., Lin, H. N., & Huang, C. H. (1990) *Biophys. J. 58*, 777–783.
Soumpasis, D. M. (1983) *Biophys. J. 41*, 95–97.
Tocanne, J. F., Dupou-Cezanne, L., Lopez, A., & Tournier, J. F. (1989) *FEBS Lett. 257*, 10–16.
Vaz, W. L. C., & Hallmann, D. (1983) *FEBS Lett. 152*, 287–290.
Vaz, W. L. C., Clegg, R. M., & Hallmann, D. (1985) *Biochemistry 24*, 781–786.
Vaz, W. L. C., Melo, E. C. C., & Thompson, T. E. (1989) *Biophys. J. 56*, 869–876.
Vaz, W. L. C., Melo, E. C. C., & Thompson, T. E. (1990) *Biophys. J. 58*, 273–275.
Xia, W., & Thorpe, M. F. (1988) *Phys. Rev. A. 38*, 2650–2656.

Serine-Specific Phosphorylation of Nicotinic Receptor Associated 43K Protein†

Joseph A. Hill, Jr., Hoâng-Oanh Nghiêm, and Jean-Pierre Changeux*
URA CNRS D1284, Neurobiologie Molêculaire, Institut Pasteur, 25, rue du Dr. Roux, Paris 75724 Cêdex 15, France
Received November 8, 1990; Revised Manuscript Received February 19, 1991

ABSTRACT: In *Torpedo marmorata* electroplaque, an extrinsic membrane protein of apparent mass 43 000 daltons colocalizes with the cytoplasmic face of the nicotinic acetylcholine receptor (AChR) in approximately 1:1 stoichiometry. We show that this 43K protein can be phosphorylated in vitro by endogenous protein kinases present in AChR-rich membranes. The extent of 43K protein phosphorylation exceeds that of the subunits of the AChR, well-established substrates for enzymatic phosphorylation. We demonstrate that significant 43K phosphoprotein exists in vivo. The kinetics of phosphate incorporation mediated by endogenous kinases differed significantly from those of the AChR subunits, suggesting that different phosphorylation cascades are involved. Use of specific inhibitors of a variety of protein kinases indicated that endogenous cAMP-dependent protein kinase catalyzes phosphorylation of the 43K protein in vitro. All of the phosphate incorporated into 43K protein was accounted for by phosphoserine (0.65 mol/mol of 43K protein). Potential structural and functional consequences of 43K protein phosphorylation are discussed.

Efficient signal transmission in the nervous system relies upon the exquisite structural specialization of the chemical synapse. The machinery for release and subsequent degradation of neurotransmitter is closely aligned with the postsynaptic receptor. At the neuromuscular junction, nicotinic acetylcholine receptors (AChRs)[1] are apposed and immobilized in densely packed clusters (≈8000/μm^2; Fertuck & Salpeter, 1974) at the crests of postjunctional folds close to the sites of acetylcholine release. The mechanism whereby this structure develops, is maintained, and is regenerated after injury are the subject of intense inquiry [recent reviews: Bloch and Pumplin (1988) and Changeux et al. 1991)].

Concentrated at the motor endplate postsynaptic membrane are a number of proteins in addition to AChR. The most prominent among these proteins, termed 43K protein for its apparent molecular mass on SDS gels, colocalizes with the AChR in close association with the cytoplasmic face of receptor clusters (Froehner et al., 1981; Sealock, 1982; Nghiêm et al., 1983; Sealock et al., 1984; Kordeli et al., 1986, 1989; Bridgman et al., 1987). First discovered in a model system, the innervated face of the *Torpedo marmorata* electrocyte (Sobel et al., 1977), the function of 43K protein has yet to be elucidated.

Some evidence suggests that 43K protein is involved in the development and maintenance of postsynaptic cytoarchitecture [recent reviews: Changeux et al. (1991) and Froehner (1986)]. Removal of 43K protein by brief exposure to alkaline pH leads to increased lateral and rotational mobility of the AChR [see Froehner (1989) for references]. 43K protein is consistently found at the cytoplasmic face of mature AChR clusters; in the absence of receptor clusters, 43K protein cannot be detected (Kordeli et al., 1986; Bloch & Pumplin, 1988). In cultured myotubes, 43K protein coaggregates with the AChR during spontaneous and experimentally induced AChR aggregation (Burden, 1985; Bloch & Froehner, 1987; Peng & Froehner, 1985). AChRs reconstituted in *Xenopus* oocytes or in fibroblasts assemble into clusters when coexpressed with 43K protein (Froehner et al., 1990; Phillips et al., 1991).

† This work was supported by the Centre National de la Recherche Scientifique, the Collège de France, the Institut National de la Santé et de la Recherche Médicale (Contract 872004), the Direction des Recherches et Etudes Techniques (Contract 87/211), the Muscular Dystrophy Association of America, and the Association Française Contre les Myopathies.
* To whom correspondence should be addressed.

[1] Abbreviations: AChR, nicotinic acetylcholine receptor; SDS, sodium dodecyl sulfate; CHAPS, 3-[(3-cholamidopropyl)dimethylammonio]-1-propanesulfonate; PAGE, polyacrylamide gel electrophoresis; BSA, bovine serum albumin; TPA, 12-*O*-tetradecanoylphorbol 13-acetate; TCA, trichloroacetic acid; DTT, dithiothreitol.

0006-2960/91/0430-5579$02.50/0